



Electron mass renormalization and absorption of hard photons

Esmaiel Pourjafarabadi^{1,a}, Amirhosein Mojavezi^{2,b}

¹ Physics Department and Biruni Observatory, Shiraz University, Shiraz 71454, Islamic Republic of Iran

² Department of Physics, University of Qom, Ghadir Blvd., Qom 371614-6611, Islamic Republic of Iran

Received: 5 December 2021 / Accepted: 9 August 2022
© The Author(s) 2022

Abstract Mass renormalization of the electron in configurations such as metallic hydride surfaces due to electromagnetic field fluctuations leads to mass enhancement of the electron, which is known as the *heavy electron*. The effective mass renormalization has substantial consequences in the theory of electromagnetic field interaction with matter (QED). One of the fascinating effects appears when an external photon interacts with the heavy electron. In this case, the wavelength of the scattered photon from the electron increases and the hard photon turns into a soft photon. In this paper, we present a novel mechanism to show how the heavy electron results in hard photon absorption.

1 Introduction

According to the perturbative field theories, one can expand n-point functions around the coupling constant in low energies. At high orders consisting of loop Feynman diagrams, the physical quantities achieve quantum radiative corrections. So, to calculate any physical quantity, such as mass, two parts contribute, namely the *bare* value that appears in the Lagrangian and quantum corrections Δm as

$$m_{Physical} = m_{bare} + \Delta m. \quad (1)$$

Because of the undetermined momentum in the loop Feynman diagrams, $m_{Physical}$ in the above equation has no definite value and diverges, called *ultraviolet divergences*. The renormalization program as an instruction controls all infinity in the whole of the theory. The renormalization program not only leads to the absorption of divergences of the amplitudes but also modifies the results of the calculation of physically observable quantities such as the mass and the electric charge.

^a e-mail: pesmaiel@yahoo.com

^b e-mail: amojaezi98@gmail.com (corresponding author)

The electron as a fundamental particle does not exist alone in real processes. Rather, it is coupled with a gauge field (the photon), known as QED theory. Beyond the leading order of QED, as mentioned earlier, electron mass and charge are modified due to quantum corrections. In this manner, in surveying any physical processes, the electrons should be considered as the *renormalized electron*, not the bare one [1, 2]. Renormalization procedures for quantities such as mass and electric charge have been very well known for many years. Mass renormalization has vital consequences in physical processes (see for instance [3, 4]). In condensed matter physics, mass renormalization is usually interpreted as mass enhancement of the particle; for example, the renormalized electron is considered a *heavy electron*.

The most serious problem with the renormalization procedure is the presence of boundary conditions on the quantum fields. The presence of the boundaries imposes crucial constraints on the propagators and for n-point functions. Here, propagators do not have the standard form (wave functions are not plane waves) and depend completely on the non-trivial properties that break translational symmetry. Therefore, all physical quantities will be modified according to symmetry breaking. Altogether, the renormalization program with nontrivial boundary conditions is complicated. However, attempts have been made in [5–8] for scalar field theory and in [9] for QED theory.

As mentioned earlier, the modification of the electron propagators due to boundary conditions (for example, in a lattice) causes that electron to become heavy. The first image of heavy electrons was captured in [10] using spectroscopic imaging scanning tunneling microscopy (SI-STM) by measuring the wavelength of electrons on the surface of the material. It was shown that under extreme conditions, electrons take large mass. In another experiment, in [11], by visualizing the electron wave in the crystal with STM, it has been shown that moving electrons in some lattices can make them more massive than the free one.

The effective mass renormalization is one of the most interesting areas and very well known in physics; for instance, superconductivity in heavy fermion material [12–16], Hall effect evolution in a heavy electron critical point [17, 18], heavy electron systems in Fermi liquid theory [19], non-Fermi liquid behavior in heavy fermion metal [20, 21], and magnetic properties of the heavy fermion [22, 23]. Recently, some notable works have emerged in this area: nonlocal Kondo effect and quantum critical phase in heavy fermion metals [24], heavy fermion thin films [25], and heavy fermions in Kondo lattice models [26]. However, in [27], the authors have also used the concept of heavy electron to explain the theory of low-energy nuclear reaction (LENR) [28–34]. According to the LENR, the electrons in the metallic hydride surfaces are subjected to the localized condensed matter electromagnetic fields. In these conditions, the proton can capture the renormalized electrons, where very low-momentum neutrons (along with neutrinos) are produced to induce chains of nuclear reactions in neighboring condensed matter [35, 36]. Usually, a proton can capture a charged lepton to produce a neutron and a neutrino.



For the above reaction, it is necessary that the following condition on the mass of the lepton is preserved (see please [37, 38]),

$$M_l > 2.53M_e^0, \quad (3)$$

where M_e^0 is the free electron mass. Equation (2) holds for the muon, but not for a free electron. In [27], the authors explain how the modification of the electron mass, yields such chain reactions. Also, the heavy electron may absorb gamma rays from nuclear reactions due to (2).

According to the crucial application of the heavy electron, especially in shielding gamma rays, it is substantial to create them anyway. In [39, 40] heavy electron can be produced from carbon nanoparticles called *nanohorn*. Because of the nanohorn structures with sharp edges, when laser light strikes them, where electric charge accumulates, they produce surface plasmons containing massive oscillations of electrons. The mass and resonance interaction of these electrons with protons or deuterons within the porous structure of the nanohorns creates a strong local electric field between electrons and protons and ultimately produces heavy electrons. In this paper, we survey the absorption of gamma rays in detail and present a novel mechanism to approve that heavy electrons can absorb gamma rays and that hard photons from nuclear reactions are turned into soft ones.

We organize this paper as follows. In Sect. 2, we very briefly discuss the procedure for the electron mass renormalization and heavy electron. We examine the renormalization of the mass as it affects the kinematics of the electron. In Sect. 3, we investigate the photon scattering from the elec-

tron in the presence of an electromagnetic field to prove the absorption of hard photons. It is Compton scattering with the difference that the bare electron is replaced with a renormalized electron. We show that the cross-section of modified Compton scattering is truly different from the usual one. Our results reduce to the standard Compton scattering when the renormalized electron is considered a free electron. In Sect. 4, we present our results.

2 Mass renormalization of the electron: a brief review

In this section, we briefly investigate the renormalization of the electron mass. Our approach is in the framework of renormalized perturbation theory. The Lagrangian for QED is

$$\mathcal{L}_{\text{QED}} = -\frac{1}{4}(F^{\mu\nu})^2 + \bar{\Psi}(i\partial^\mu - m_0)\Psi - e_0\bar{\Psi}\gamma_\mu\Psi A^\mu. \quad (4)$$

where m_0 and e_0 are the bare mass and the bare electric charge, respectively. $\Psi(x)$ and $A^\mu(x)$ are fermion and photon fields, respectively, and can be written as

$$\Psi(x) = \int \frac{d^3p}{(2\pi)^3} \sum_{s=1,2} \frac{1}{\sqrt{2E_p}} \left[c_p^s \psi^s(x) + d_p^{s\dagger} \phi^s(x) \right] \quad (5)$$

$$A_\mu(x) = \int \frac{d^3p}{(2\pi)^3} \sum_{s=0}^3 \frac{1}{\sqrt{2\omega_p}} \left[a_p^s \tilde{A}_\mu^s(x) + a_p^{s\dagger} \tilde{A}_\mu^{s*}(x) \right], \quad (6)$$

where, in the first line, $c_p^{s\dagger}$ (c_p^s) and $d_p^{s\dagger}$ (d_p^s) create (annihilate) a fermion and anti-fermion with momentum p and spin direction s , respectively. Here, $\psi^s(x)$ and $\phi^s(x)$ are the particle and anti-particle solutions of the Dirac equation, respectively. In the second line, $a_p^{s\dagger}$ (a_p^s) creates (annihilates) a photon with momentum p and polarization $\varepsilon_\mu^s(p)$, and $\tilde{A}_\mu^s(x)$ are the momentum-space solution of the equation $\partial^\mu A_\mu = 0$.

According to the above, the electron propagator (Green's function $G(p)$) takes some corrections and can be written in perturbative series of QED as [41]:

$$iG(p) = \frac{p}{p - m_0} + \frac{p}{p - m_0} \left(i\Sigma_2(p) \right) \frac{p}{p - m_0} + \frac{p}{p - m_0} \left(i\Sigma_2(p) \right) \frac{p}{p - m_0} \left(i\Sigma_2(p) \right) \frac{p}{p - m_0} + \dots \quad (7)$$

$$iG(p) = \frac{i}{p - m_0} + \frac{i}{p - m_0} \left(i\Sigma_2(p) \right) \frac{i}{p - m_0} + \frac{i}{p - m_0} \left(i\Sigma_2(p) \right) \frac{i}{p - m_0} \left(i\Sigma_2(p) \right) \frac{i}{p - m_0} + \dots, \quad (8)$$

where, in Feynman gauge,

$$i\Sigma_2(\not{p}) = (-ie)^2 \int \frac{d^4k}{(2\pi)^4} \gamma^\mu \frac{i(\not{k} + m_0)}{k^2 - m_0^2 + i\epsilon} \gamma^\mu \frac{-i}{(p - k)^2 + i\epsilon}, \quad (9)$$

is known as *electron self energy*. Equation (9) is a part of some geometric series. One can rewrite that

$$iG(\not{p}) = \frac{i}{\not{p} - m_0 - \Sigma_2(\not{p})}. \quad (10)$$

It is obvious that the pole of the propagator is shifted away from m_0 by $\Sigma_2(\not{p})$. In fact, The $\Sigma_2(\not{p})$ as a radiative correction modifies not only the propagator but also the bare mass of the electron and results in *Renormalized mass* m_R :

$$m_R = m_0 + \Sigma_2(\not{p}). \quad (11)$$

Up to now, the renormalization program has been done in momentum space. However, if the translational invariance of the system breaks strongly, then the momentum is no longer a good quantum number. Renormalization in configuration space can be applied for such a situation, such as in problems with a nontrivial BC or a nonzero background that cannot be treated as small perturbations. For example, the kink as a constant background in 1+1 dimensions breaks the translational invariance, or in the Casimir effect, we have nontrivial BC on the walls. Another real example of QED is the Lamb shift in which the Coulomb potential in the hydrogen atom breaks the translational symmetry. We present a systematic treatment, up to order α , for the renormalization of quantum electrodynamics in real space, especially for electron mass.

By replacing $\Psi(x) = \sqrt{z_2}\Psi_r(x)$ and $A^\mu(x) = \sqrt{z_3}A_r^\mu(x)$ in (4), we have

$$\mathcal{L}_{\text{QED}} = -\frac{1}{4}z_3(F_r^{\mu\nu})^2 + z_2\bar{\Psi}_r(i\not{p} - m_0)\Psi_r - e_0z_2\sqrt{z_3}\bar{\Psi}_r\gamma_\mu\Psi_rA_r^\mu, \quad (12)$$

where z_2 and z_3 are the field-strength renormalization for Ψ and A^μ , respectively. We define a scaling factor z_1 as $ez_1 = e_0z_2\sqrt{z_3}$ and split each term of the Lagrangian into two pieces

$$\mathcal{L}_{\text{QED}} = -\frac{1}{4}(F_r^{\mu\nu})^2 + \bar{\Psi}_r(i\not{p} - m)\Psi_r - e\bar{\Psi}_r\gamma^\mu\Psi_rA_r^\mu - \frac{1}{4}\delta_3(F_r^{\mu\nu})^2 + i\delta_2\bar{\Psi}_r\not{p}\Psi_r - (\delta_m + m\delta_2)\bar{\Psi}_r\Psi_r - e\delta_1\bar{\Psi}_r\gamma_\mu\Psi_rA_r^\mu, \quad (13)$$

with $z_3 = 1 + \delta_3$, $z_2 = 1 + \delta_2$, $m_0 = m + \delta_m$ and $z_1 = 1 + \delta_1$, where δ_1 , δ_2 , δ_3 and δ_m are counterterms. In the calculations of the quantum radiative corrections physical quantity, say electron mass, one usually encounters counterterms and the electron mass becomes renormalized. Here, m and e are the

physical mass and charge of the electron (renormalized quantities) measured at large distances. Now, the Feynman rules from the above Lagrangian for fermion fields are

$$\overrightarrow{p} = \frac{i}{\not{p} - m + i\epsilon} \quad (14)$$

$$\overrightarrow{\otimes} = i(\not{p}\delta_2 - \delta_m - m\delta_2). \quad (15)$$

We use the following notation:

$$\overrightarrow{\text{1PI}} = -i\Sigma(\not{p}) \quad (16)$$

Here, “1PI” denotes a *one-particle irreducible* diagram, which is the sum of any diagram that cannot be split in two by removing a single line. To fix the pole of the fermion propagator at the physical mass m we need two renormalization conditions:

$$\Sigma(\not{p} = m) = 0 \quad (17)$$

$$\left. \frac{d\Sigma(\not{p})}{d\not{p}} \right|_{\not{p}=m} = 0. \quad (18)$$

Now, using the dimensional regularization we can compute $-i\Sigma(\not{p})$. Applying the above renormalization conditions, up to leading order in α , the divergent parts of the counterterms is derived as

$$\delta_2 \sim -\frac{e^2}{8\pi^2\epsilon}, \quad (19)$$

$$\delta_m \sim -\frac{3me^2}{8\pi^2\epsilon}, \quad (20)$$

where $d = 4 - \epsilon$ is the spacetime dimension so that we should take the limit $\epsilon \rightarrow 0$. These counterterms can remove all UV divergences of the QED theory for a fermion propagator in free space.

According to the Lagrangian (13), the perturbation expansion of the full electron propagator up to order α is

$$\begin{aligned} -i\Sigma &= \bullet - \text{1PI} = \bullet - \text{1PI} \\ &+ \bullet - \text{1PI} + \bullet - \text{1PI} \end{aligned} \quad (21)$$

We choose our renormalization condition in such a way that the pole of the first term of the right-hand side (RHS) gives

the physical mass m at $x = x_0$. It requires that the sum of remaining diagrams, which we call $-i\tilde{\Sigma}(x)$, vanishes at this point, namely

$$\begin{aligned} -i\tilde{\Sigma}(x) \Big|_{x=x_0} &= \left(\text{---} \begin{array}{c} \text{---} \\ x \\ \text{---} \end{array} \text{---} \begin{array}{c} \text{---} \\ y \\ \text{---} \end{array} \text{---} + \text{---} \begin{array}{c} \text{---} \\ x \\ \text{---} \end{array} \text{---} \otimes \text{---} \begin{array}{c} \text{---} \\ x \\ \text{---} \end{array} \text{---} \right)_{x=x_0} \\ &= 0, \quad \text{and} \quad \frac{d[-i\tilde{\Sigma}(x)]}{dx} \Big|_{x=x_0} = 0. \end{aligned} \quad (22)$$

We can write $-i\tilde{\Sigma}$ to order α as

$$\begin{aligned} -i\tilde{\Sigma}(x) &= \int d^d y \bar{\psi}(y) [-i\Sigma_2(x, y)] \psi(x) + \bar{\psi}(x) \\ &\quad \times [-\delta_2(x)\not{p} - im\delta_2(x) - i\delta_m(x)] \psi(x) \end{aligned} \quad (23)$$

Thus, the first condition in Eq. (22) yields

$$\begin{aligned} -i\tilde{\Sigma}(x_0) &= \left\{ \int d^d y \bar{\psi}(y) [-i\Sigma_2(x, y)] \psi(x) + \bar{\psi}(x) \right. \\ &\quad \times [-\delta_2(x)\not{p} - im\delta_2(x) - i\delta_m(x)] \psi(x) \Big\}_{x=x_0} \end{aligned} \quad (24)$$

$$= 0, \quad (25)$$

where $-i\Sigma_2$ is $O(\alpha)$ electron self-energy diagram. Now, using the Dirac equation $(i\not{p} - m)\psi = 0$, up to order α we obtain

$$\delta_m = \frac{-1}{\bar{\psi}(x_0)\psi(x_0)} \int d^d y \bar{\psi}(y) \Sigma_2(x, y) \psi(x) \Big|_{x=x_0}. \quad (26)$$

δ_m corresponds to $\Sigma_2(p)$ up to order α , but for the case that translational symmetry may be broken. It is obvious that δ_m depends on the boundary conditions of the fields. Thus, quantum correction of the electron mass depends on nontrivial properties that break translational symmetry. It is customary in condensed matter physics that the impact of $\delta_m(x)$ on the mass would have been considered a heavy electron (see [42–47] for heavy electron theory). For instance, in interaction $p + e \rightarrow n + \nu$, ignoring ν mass, we have

$$\Delta m = (M_n - M_p - M_e)c^2 \approx 0.78 \text{ MeV}. \quad (27)$$

$$m_e^* = m_e + 0.78 \text{ MeV} = 2.53m_e \quad (28)$$

This value is especially important in LENR interactions in the hydrogen-metal environment that lead to the production of ultra-low energy neutrons and nuclear transmutation. In [27], it is stressed that the minimum of the mass growth parameter $\beta = \frac{m_R}{m_0}$ for reaction $p + e^* \rightarrow n + \nu$ is $\beta = 2.53$; e^* denotes heavy electron. In the next section, we will show how heavy electron via Compton scattering leads to absorption of the gamma rays.

3 Absorption of gamma rays: revisited Compton scattering

In this section, we survey the photon scattering of the electron surrounded by electromagnetic fields produced by the oscillating protons near them. In this case, the electron does not obey the Dirac equation, while it is considered as a renormalized electron that we have referred to. We will show that these renormalized electrons can absorb hard photons produced in nuclear reactions, changing them to the soft ones. Compton scattering is the scattering of a photon after an interaction with a charged particle (preferably an electron here). However, we model such photon scattering from the surface renormalized electron in a metal, noting that X-ray photon energy (of order 17 keV) is much higher than the binding energy in the atom, which seems logical.

Two Feynman diagrams contribute to the M-matrix for Compton scattering as follows (for more details, see [48]):

$$\begin{aligned} iM &= \text{---} \begin{array}{c} \text{---} \\ e \\ \text{---} \end{array} \text{---} \begin{array}{c} \text{---} \\ \gamma \\ \text{---} \end{array} \text{---} \begin{array}{c} \text{---} \\ e \\ \text{---} \end{array} \text{---} \begin{array}{c} \text{---} \\ \gamma \\ \text{---} \end{array} \\ &+ \text{---} \begin{array}{c} \text{---} \\ e \\ \text{---} \end{array} \text{---} \begin{array}{c} \text{---} \\ \gamma \\ \text{---} \end{array} \text{---} \begin{array}{c} \text{---} \\ e \\ \text{---} \end{array} \text{---} \begin{array}{c} \text{---} \\ \gamma \\ \text{---} \end{array} \end{aligned} \quad (29)$$

$$\begin{aligned} iM &= -ie^2 \epsilon_\mu^*(q') \epsilon_\nu(q) \bar{u}(p') \left(\frac{\gamma^\mu (\not{p} + \not{q} + m_0) \gamma^\nu}{(p + q)^2 - m_0^2} \right. \\ &\quad \left. + \frac{\gamma^\nu (\not{p} + \not{q} + m_0) \gamma^\mu}{(p - q')^2 - m_0^2} \right) u(p), \end{aligned} \quad (30)$$

where p (p') and q (q') represent internal (external) momenta of the electron and photon, respectively, and ϵ_μ^* (ϵ_μ) shows the polarization of the output (input) photon. Doing some trace technologies, summing over all spins and polarizations, when the smoke clears, one can derive (see appendix for details)

$$\begin{aligned} \frac{1}{4} \sum_{\text{spins}} |M|^2 = & \frac{16e^4}{4} \left(\frac{4m_0^2 m_R^2 - 2m_R^2(p.p') + 4m_0^2(p.q) - 2m_R^2(p'.q) + 2(p.q)(p'.q)}{(m_R^2 - 2p.q - m_0^2)^2} \right. \\ & + 2 \frac{-2(p.p')(q.q') + 2(p'.p)(q.p) - m_R^2(p'.q) - m_R^2(p'.q') - m_R^2(p'.p)}{(m_R^2 - 2p.q - m_0^2)(m_R^2 - 2p.q' - m_0^2)} \\ & + 2 \frac{-2(p.p')(p.q') + m_0^2(q'.q) - 2m_0^2(p.q) + 2m_0^2(p.q') - 4m_0^2 m_R^2}{(m_R^2 - 2p.q - m_0^2)(m_R^2 - 2p.q' - m_0^2)} \\ & \left. + \frac{4m_0^2 m_R^2 - 2m_R^2(p.p') - 4m_0^2(p.q) + 2m_R^2(p'.q') + 2(p.q')(p'.q')}{(m_R^2 - 2p.q' - m_0^2)^2} \right). \end{aligned} \quad (31)$$

Please note that in the above equation, m_0 (an electron which obeys the Dirac equation) differs from m_R (heavy electron). The momentum of the electron subjected to the electromagnetic field is $P_\mu = p_\mu - eA_\mu$, where P_μ is the momentum of an electron interacting with gauge vector field A_μ . Thus, we would have concluded that $(p_\mu - eA_\mu)(p^\mu - eA^\mu) = m_R^2$. To turn Eq. (31) into a cross-section, both a picture of the kinematics and the reference frame of Compton scattering must be considered. Choosing the lab frame in which the electron is initially at rest, and $q = (\omega, \omega\hat{z})$, $p = (m_R, 0)$, $q' = (\omega', \omega' \sin \theta, 0, \omega' \cos \theta)$ and $p' = (E', \mathbf{P}')$, altogether, we take,

$$\begin{aligned} \frac{1}{4} \sum_{\text{spins}} |M|^2 = & 4e^4 \left(\frac{4m_0^2 m_R^2 - 2m_R^2(m_R^2 + \omega\omega'(1 - \cos \theta)) + 4m_0^2 m_R^2 \omega - 2m_R^3 \omega' + 2m_R^2 \omega \omega'}{(m_R^2 - 2m_R \omega - m_0^2)^2} \right. \\ & + 2 \frac{-2\omega\omega'(1 - \cos \theta)(m_R^2 + \omega\omega'(1 - \cos \theta)) + 2m_R \omega(m_R^2 + \omega\omega'(1 - \cos \theta))}{(m_R^2 - 2m_R \omega - m_0^2)(m_R^2 - 2m_R \omega' - m_0^2)} \\ & + 2 \frac{-m_R^3 \omega' - 2m_R \omega'(m_R^2 + \omega\omega'(1 - \cos \theta)) + m_R^3 \omega - m_R^2(m_R^2 + \omega\omega'(1 - \cos \theta))}{(m_R^2 - 2m_R \omega - m_0^2)(m_R^2 - 2m_R \omega' - m_0^2)} \\ & + 2 \frac{m_R^2 \omega \omega'(1 - \cos \theta) - 2m_0^2 m_R \omega + 2m_0^2 m_R \omega' - m_R^2 m_0^2}{(m_R^2 - 2m_R \omega - m_0^2)(m_R^2 - 2m_R \omega' - m_0^2)} \\ & \left. + \frac{4m_0^2 m_R^2 - 2m_R^2(m_R^2 + \omega\omega'(1 - \cos \theta)) - 4m_0^2 m_R \omega' + 2m_R^3 \omega + 2m_R^2 \omega \omega'}{(m_R^2 - 2m_R \omega - m_0^2)^2} \right). \end{aligned} \quad (32)$$

One can calculate the differential cross-section as follows:

$$\frac{d\sigma}{d\cos \theta} = \frac{1}{8\pi} \left(\frac{\omega'}{\omega m_R} \right)^2 \left(\frac{1}{4} \sum_{\text{spins}} |M|^2 \right). \quad (33)$$

Replacing Eq. (32) in Eq. (33) with $m_R = m_0$, our result is compatible with *Klein–Nishina formula*, originally first derived in 1929 [49],

$$\frac{d\sigma}{d\cos \theta} = \frac{\pi \alpha^2}{m^2} \left(\frac{\omega'}{\omega} \right)^2 \left(\frac{\omega'}{\omega} + \frac{\omega}{\omega'} - \sin^2 \theta \right). \quad (34)$$

Defining $S = \frac{d\sigma}{d\cos \theta}$, one can calculate the energy distribu-

tion of scattered photons as follows:

$$\log(\text{count}) = \log \left(\frac{S(\omega'_i)}{\sum_{i=1} S(\omega'_i)} \right). \quad (35)$$

In Fig. 1, we show the accordance of the Klein–Nishina formula (standard Compton scattering) and our results when $m_R = m_0$.

In 2004, the Piantelli group [50] surveyed the energy distribution of scattered photons from an experiment done in the Ni-H medium (see the right side of Fig. 2). Noting that there are circumstances for LENR in the Ni-H medium,

one can expect the existence of gamma rays. However, this figure shows that the gamma radiation exists in the region below 1 MeV. Namely, despite the expectation that there is some gamma-ray radiation, gamma-ray radiation has not been detected. This is one of the interesting properties of LENR physics, which occurs mostly near metal hydride surfaces. Similar results were observed in [51]. The results of our calculations Eq. (32) on the gamma scattering of heavy electrons, as can be seen in Fig. 2, are in relative agreement with these observations. In other words, according to our calculations, the energy distribution of scattered photons from heavy electrons is in the region below 1 MeV. Absorption of the hard photons is of the characteristics of the heavy electrons in LENRs. The important point stated later, the thresh-

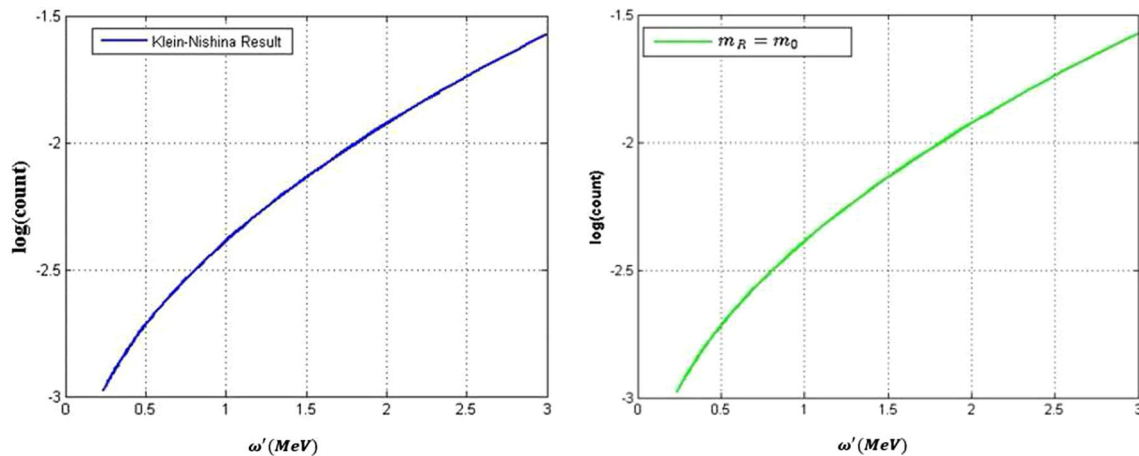


Fig. 1 Energy distribution of scattered photons ω' : Klein–Nishina formula (left), our result with $m_R = m_0$ (right)

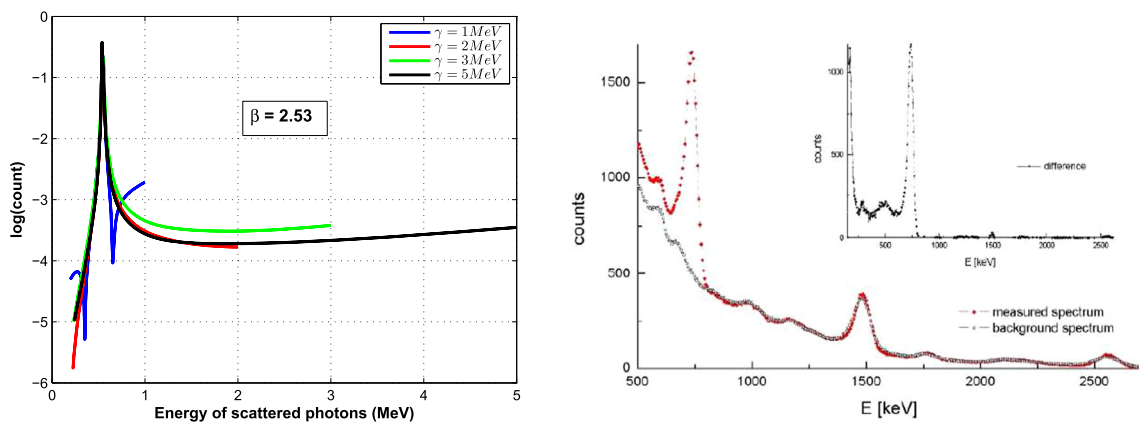


Fig. 2 Gamma-ray and heavy electron cross-section: a peak under 1 MeV for various energies of an incident photon compatible with experimental data (left). The effects of gamma radiation in the region below 1 MeV from the result of the Piantelli group [50] (right)

old enhancement of the electron mass for beginning LENRs in metal hydride surfaces and absorption of hard photons of electrons, is $m_e^* = 2.53m_e$. More precisely, opposite to Fig. 1, the peak behavior of Figs. 2 and 3 is due to the renormalization of the electron mass which is 2.53 times the original electron mass dominated by Eq. (31).

However, one can survey photon scattering angles over a range of energies. We observe that the angular distribution of scattered photons for standard Compton scattering is shown on the right side in Fig. 3: photons with energy of 1 keV and 100 keV will scatter over all angles, and photons with energy of 3 MeV and 10 MeV almost exclusively exhibit forward scattering. On the other hand, for modified Compton scattering, this distribution is not isotropic, and forward scattering is seen with photons in some specific angles (left side in Fig. 3), which may also explain why gamma-rays are not observed in some experiments.

4 Conclusion

Enhancement of the electron mass has substantial consequences in different areas of physics, especially in condensed matter, atomic, and particle physics. When an electron in some special conditions is under some electromagnetic field (EM), EM oscillations lead to heavy electrons. This can happen in the Kondo lattice or when we load protons sufficiently and appropriately on metallic hydride surfaces. In these conditions, the electrons are treated as renormalized particles with excess mass, and their physics is far from the free one. As a fascinating application of the heavy electron, we have shown that hard photons scattered from the heavy electron, according to Compton scattering, are turned into soft gamma photons. Our results are completely coincident with experimental observations: the peaks of Fig. 2 near 1 MeV conform with experiments [50, 51]. Numerous efforts have been made over many years to control and absorb high-energy gamma-

Fig. 3 Angular distribution of scattered photons from heavy electron in Eq. (34) (left). Angular distribution of scattered photons for Klein–Nishina formula (right) over a range of commonly encountered energies

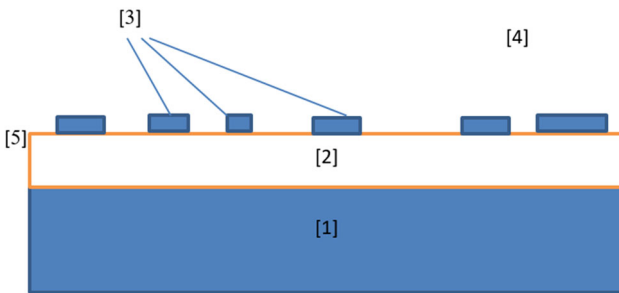
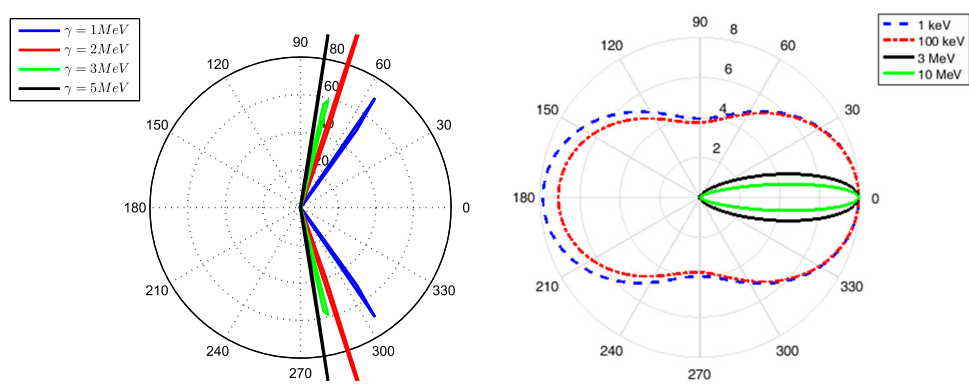


Fig. 4 Schematic of the basic design of a shield system by heavy electrons, the explanation of different parts is provided in Conclusion section

rays, and many gamma-ray shielding materials (for example, thick layers of lead) have been introduced. It is clear that the limitations of this include construction. This work presents a new field in gamma-ray absorption systems to scientists.

In Fig. 4, we propose a system of gamma-ray absorption. For area (2), which forms the surface hydride, the first step is to load 90–99% pure hydrogen or deuterium into the hydride metal surface. This metal can be palladium, nickel, or titanium. Ways to apply this load include pressure differences, chemical potential differences, or electromechanical potentials on the surface. When the hydride metal body is well loaded, the ratio of H or D to the number of atoms of the hydride body should reach 0.8 or more. At this level, the protons and deuterons slowly exit and form positively charged fragments, segment (3), on the surface (5) of the metal hydride surface. These surface patches of protons or deuterons are 1 to 10 microns in diameter and are randomly distributed on the surface. When these pieces are formed, the protons and deuterons in them begin to oscillate. Energy can then travel between the proton, deuteron, and electron sea of the surface plasmon polariton (SPP). Coupling between SPP electrons and proton-deuteron regions can increase the electric field strength near (3) fragments. As the intensity of the local electric field in these fragments increases, the mass of the local electrons in the SPP increases. Thus, heavy electrons are formed in the vicinity of zones (3). The SPP electrons in and around the regions can be heavy, but those

placed far from the zones will not be heavy. Note that the base layer (1) should be able to form a strong bond with the metal surface of the base (2) and also be a suitable thermal conductor.

Data Availability Statement This manuscript has no associated data or the data will not be deposited. [Authors' comment: The authors confirm that the data supporting the findings of this study are available within the article.]

Open Access This article is licensed under a Creative Commons Attribution 4.0 International License, which permits use, sharing, adaptation, distribution and reproduction in any medium or format, as long as you give appropriate credit to the original author(s) and the source, provide a link to the Creative Commons licence, and indicate if changes were made. The images or other third party material in this article are included in the article's Creative Commons licence, unless indicated otherwise in a credit line to the material. If material is not included in the article's Creative Commons licence and your intended use is not permitted by statutory regulation or exceeds the permitted use, you will need to obtain permission directly from the copyright holder. To view a copy of this licence, visit <http://creativecommons.org/licenses/by/4.0/>.

Funded by SCOAP³. SCOAP³ supports the goals of the International Year of Basic Sciences for Sustainable Development.

Appendix

In this section, we survey the derivation of (31) in detail. According to (30),

$$iM = -ie^2\epsilon_\mu^*(q')\epsilon_\nu(q)\bar{u}(p')\left(\frac{\gamma^\mu(\not{p} + \not{q} + m_0)\gamma^\nu}{(p+q)^2 - m_0^2} + \frac{\gamma^\nu(\not{p} + \not{q} + m_0)\gamma^\mu}{(p-q')^2 - m_0^2}\right),$$

Replacing the prescription

$$\sum_{\text{polarizations}} \epsilon_\mu^* \epsilon_\nu \rightarrow -g_{\mu\nu}, \quad (36)$$

One may easily find

$$\frac{1}{4} \sum_{\text{spins}} |M|^2 = \frac{e^4}{4} \left(\frac{A}{(p+q)^2 - m^2} \right)$$

$$\begin{aligned}
& + \frac{B}{((p+q)^2 - m^2)((p-q')^2 - m^2)} \\
& + \frac{C}{((p-q')^2 - m^2)(p+q)^2 - m^2)} \\
& + \frac{D}{(p-q')^2 - m^2} \Big), \tag{37}
\end{aligned}$$

where

$$A = \text{tr} \left((p' + m_0)(\gamma^\mu q \gamma^\nu + 2\gamma^\mu p^\nu)(\not{p} + m_0) \right. \\
\left. (\gamma_\nu q \gamma_\mu + 2\gamma_\mu p_\nu) \right)$$

$$B = \text{tr} \left((p' + m_0)(\gamma^\mu q \gamma^\nu + 2\gamma^\mu p^\nu)(\not{p} + m_0) \right. \\
\left. (-2\gamma_\nu p_\mu + \gamma_\mu q / \gamma_\nu) \right)$$

A, B, C, and D are complicated traces. Noting that replacing q with q' we get $A = D$, and also, due to the ability to reverse the order of the γ matrices we have $B = C$, here we only survey the trace terms for A, and the other terms are similar. There are 16 separate trace terms for each numerator. We choose one of them, for instance

$$\begin{aligned}
\text{tr}(2p/\gamma^\mu q \gamma^\nu \not{p} \gamma_\mu p_\nu) &= 2 \text{tr}(p'_\lambda \gamma^\lambda \gamma^\mu q_s \gamma^s \gamma^\nu p_t \gamma^t \gamma_\mu p_\nu) \\
&= -4 \text{tr}(\gamma^\lambda \gamma^\nu \gamma^t \gamma^s) \\
&= -4 p'_\lambda p_\nu p_t q_s (4[g^{\lambda t} g^{\nu s} - g^{\lambda \nu} g^{\nu s} \\
&\quad + g^{\lambda s} g^{\nu t}]) \\
&= -16 ((p \cdot p)(p \cdot q) - (p \cdot p')(p \cdot q) \\
&\quad + (p' \cdot q)(p \cdot p)) \\
&= -16 m_R^2 (p' \cdot q),
\end{aligned}$$

References

1. J. Schwinger, Electron anomaly to order α . *Phys. Rev.* **73**, 416 (1948)
2. F.J. Dyson, The radiation theories of Tomonaga, Schwinger, and Feynman. *Phys. Rev.* **75**, 486 (1949)
3. J. Fröhlich, A. Pizzo, Renormalized electron mass in nonrelativistic QED. *Commun. Math. Phys.* **294**, 439–470 (2010)
4. Feliciano Giustino, Electron-phonon interactions from first principles. *Rev. Mod. Phys.* **91**, 019901 (2019)
5. R. Moazzemi, S.S. Gousheh, A new renormalization approach to the Dirichlet Casimir effect for 4 theory in (1+1) dimensions. *Phys. Lett. B* **658**, 255 (2008)
6. S.S. Gousheh, R. Moazzemi, M.A. Valuyan, Radiative correction to the Dirichlet Casimir energy for 4 theory in two spatial dimensions. *Phys. Lett. B* **681**, 477 (2009)
7. R. Moazzemi, M. Namdar, S.S. Gousheh, The Dirichlet Casimir effect for 4 theory in (3+1) dimensions: a new renormalization approach. *JHEP* **09**, 029 (2007)
8. M.A. Valuyan, Radiative correction to the Casimir energy with mixed boundary condition in 2 + 1 dimensions. *Indian J. Phys.* (2020). <https://doi.org/10.1007/s12648-020-01758-8>
9. A. Mojavezi, R. Moazzemi, Coordinate space representation for renormalization of quantum electrodynamics. *EPJP* **136**, 200 (2021)
10. A.R. Schmidt, M.H. Hamidian, P. Wahl, F. Meier, A.V. Balatsky, J.D. Garrett, T.J. Williams, G.M. Luke, J.C. Davis, Imaging the Fano lattice to hidden order transition in URu_2Si_2 . *Nature* 09073 (2010)
11. P. Aynajian, E.H. da Silva Neto, A. Gyenis, R.E. Baumbach, J.D. Thompson, Z. Fisk, E.D. Bauer, A. Yazdani, Visualizing heavy fermions emerging in a quantum critical Kondo lattice. *Nature* **486**(7402), 201–206 (2012)
12. Y.F. Yang, D. Pines, Emergence of superconductivity in heavy-electron materials. *Proc. Natl. Acad. Sci.* **111**(51), 18178–18182 (2014)
13. Y.F. Yang, D. Pines, Emergence of superconductivity in heavy-electron materials. *Proc. Natl. Acad. Sci.* **111**(51), 18178–18182 (2014)
14. C. Broholm, J.K. Kjems, W.J.L. Buyers, P. Matthews, T.T.M. Palstra, A.A. Menovsky, J.A. Mydosh, Magnetic excitations and ordering in the heavy-electron superconductor URu_2Si_2 . *Phys. Rev. Lett.* **58**(14), 1467 (1987)
15. N.D. Mathur, F.M. Grosche, S.R. Julian, I.R. Walker, D.M. Freye, R.K.W. Haselwimmer, G.G. Lonzarich, Magnetically mediated superconductivity in heavy fermion compounds. *Nature* **394**(6688), 39–43 (1998)
16. G.E. Volovik, L.P. Gor'kov, Superconducting classes in heavy-fermion systems. In *30 Years of the Landau Institute-Selected Papers* (pp. 258–269) (1996)
17. S. Paschen, T. Lühmann, S. Wirth, P. Gegenwart, O. Trovarelli, C. Geibel, F. Steglich, P. Coleman, Q. Si, Hall-effect evolution across a heavy-fermion quantum critical point. *Nature* **432**(7019), 881–885 (2004)
18. S. Nair, S. Wirth, S. Friedemann, F. Steglich, Q. Si, A.J. Schofield, Hall effect in heavy fermion metals. *Adv. Phys.* **61**(5), 583–664 (2012)
19. A. Auerbach, K. Levin, Kondo bosons and the Kondo lattice: microscopic basis for the heavy Fermi liquid. *Phys. Rev. Lett.* **57**(7), 877 (1986)
20. G.R. Stewart, Non-Fermi-liquid behavior in d-and f-electron metals. *Rev. Mod. Phys.* **73**(4), 797 (2001)
21. H.V. Löhneysen, T. Pietrus, G. Portisch, H.G. Schlager, A. Schröder, M. Sieck, T. Trappmann, Non-Fermi-liquid behavior in a heavy-fermion alloy at a magnetic instability. *Phys. Rev. Lett.* **72**(20), 3262 (1994)
22. T.T.M. Palstra, A.A. Menovsky, J. Van den Berg, A.J. Dirkmaat, P.H. Kes, G.J. Nieuwenhuys, J.A. Mydosh, Superconducting and magnetic transitions in the heavy-fermion system URu_2Si_2 . *Phys. Rev. Lett.* **55**(24), 2727 (1985)
23. A. Schröder, G. Aeppli, R. Coldea, M. Adams, O. Stockert, H. Löhneysen, E. Bucher, R. Ramazashvili, P. Coleman, Onset of antiferromagnetism in heavy-fermion metals. *Nature* **407**(6802), 351–355 (2000)
24. J. Wang, Y.F. Yang, Nonlocal Kondo effect and quantum critical phase in heavy-fermion metals. *Phys. Rev. B* **104**(16), 165120 (2021)
25. S. Chatterjee, Heavy fermion thin films: progress and prospects. *Electron. Struct.* **3**, 043001 (2021)
26. B. Danu, Z. Liu, F.F. Assaad, M. Raczkowski, Zooming in on heavy fermions in Kondo lattice models. *arXiv preprint arXiv:2107.10272* (2021)
27. A. Widom, L. Larsen, Ultra low momentum neutron catalyzed nuclear reactions on metallic hydride surfaces. *Eur. Phys. J. C* **46**, 107–111 (2006)
28. T. Mizuno, Experimental confirmation of the nuclear reaction at low energy caused by electrolysis in the electrolyte. In *Proceedings*

for the Symposium on Advanced Research in Energy Technology (2000)

- 29. E. Storms, *Science of Low Energy Nuclear Reaction: A Comprehensive Compilation of Evidence and Explanations about Cold Fusion* (World Scientific, Singapore, 2007)
- 30. T. Mizuno, Observation of excess heat by activated metal and deuterium gas. *J. Condens. Matter Nucl. Sci.* **25**, 1–25 (2017)
- 31. T. Mizuno, J. Rothwell, Excess heat from palladium deposited on nickel. *J. Condens. Matter Nucl. Sci.* **29**, 21–33 (2019)
- 32. Y. Iwamura, T. Itoh, M. Sakano, S. Sakai, Observation of low energy nuclear reactions induced by D2 gas permeation through Pd complexes. *Proc. of ICCF9* (2002)
- 33. I.M. Kadenko, N.V. Sakhno, Possible LENR observation due to dineutron formation as a product of the $^{159}\text{Tb}(n, 2n)^{158}\text{Tb}$ nuclear reaction. *Acta Phys. Polon. B* **51**, 83 (2020)
- 34. P. Kálmán, T. Keszthelyi, Forbidden nuclear reactions. *Phys. Rev. C* **99**(5), 054620 (2019)
- 35. D.R. Lide (ed.), *Handbook of Chemistry and Physics, Sect. 11*, 81st edn. (CRC Press, Boca Raton, 2000)
- 36. R. Firestone, V. Shirley (eds.), *Table of Radioactive Isotopes* (Wiley, New York, 1999)
- 37. L.D. Landau, E.M. Lifshitz, *The Classical Theory of Fields, Sects. 17 and 47, Prob. 2* (Pergamon Press, Oxford, 1975)
- 38. V.B. Berestetskii, E.M. Lifshitz, L.P. Pitaevskii, *Quantum Electrodynamics, Sect. 40, Eq. (40.15)* (Butterworth Heinemann, Oxford, 1997)
- 39. J.M. Zawodny, National Aeronautics and Space Administration NASA, Method for Producing Heavy Electrons. U.S. Patent Application 13/070,552 (2011)
- 40. M. Schiavon, Method for the producing heavy electrons, European Patent Office, EP3076396A1 (2018)
- 41. M.D. Schwartz, *Quantum Field Theory and the Standard Model* (Cambridge University Press, Cambridge, 2014)
- 42. A.O. Barut, P. Cordero, G.C. Ghirardi, Theory of the heavy electron. *Phys. Rev.* **182**(5), 1844 (1969)
- 43. P.A. Lee, T.M. Rice, J.W. Serene, L.J. Sham, J.W. Wilkins, Theories of heavy-electron systems. *Comments Condens. Matter Phys.* **12**(3), 99–161 (1986)
- 44. Y.F. Yang, D. Pines, Universal behavior in heavy-electron materials. *Phys. Rev. Lett.* **100**(9), 096404 (2008)
- 45. N. Tsujii, H. Kontani, K. Yoshimura, Universality in heavy fermion systems with general degeneracy. *Phys. Rev. Lett.* **94**(5), 057201 (2005)
- 46. L. Degiorgi, The electrodynamic response of heavy-electron compounds. *Rev. Mod. Phys.* **71**(3), 687 (1999)
- 47. S.G. Stewart, Heavy-fermion systems. *Rev. Mod. Phys.* **56**(4), 755 (1984)
- 48. M.E. Peskin, D.V. Schroeder, *An Introduction to Quantum Field Theory* (Avalon Publishing, New York, 1995)
- 49. O. Klein, Y. Nishina, *Z. Phys.* **52**, 853 (1929)
- 50. S. Focardi et al., Evidence of electromagnetic radiation from Ni-H Systems. In *Eleventh International Conference on Condensed Matter Nuclear Science*, Marseille (2004)
- 51. Y. Iwamura, T. Itoh, S. Tsuruga, J. Condens. Matter Nucl. Sci. **13**, 242–252 (2014)